A Revisit of Delayed Yield Phenomenon in Unconfined Aquifer

Deqiang Mao, Li Wan, Tian-Chyi J. Yeh, Cheng-Haw Lee, Kuo-Chin Hsu, Jet-Chau Wen, and Wenxi Lu

Water Resour. Res. **doi:10.1029/2010WR009326,2011**

National Central University, Taiwan, ROC. 11/21/2014

Unconfined Aquifer Pumping Test

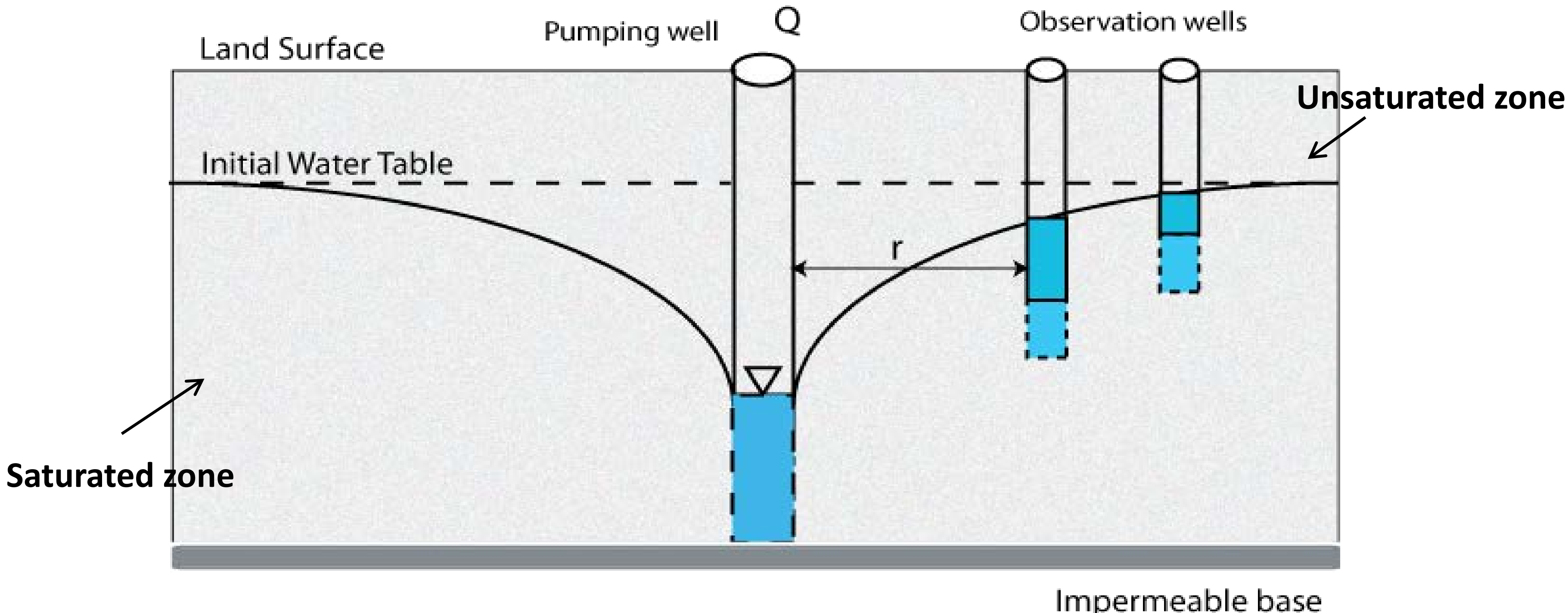

Variably saturated governing equation

$$\nabla \cdot [K(h,\mathbf{x})\nabla(h+z)] = \omega S_s(\mathbf{x})\frac{\partial h}{\partial t} + \frac{\partial \theta}{\partial t} = \left(\omega S_s(\mathbf{x}) + C(h,\mathbf{x})\right)\frac{\partial h}{\partial t}$$

$$K(h) = K_s \exp(\alpha h)$$

$$\theta(h) = \theta_r + (\theta_s - \theta_r)\exp(\beta h)$$

S-shaped Drawdown Curve

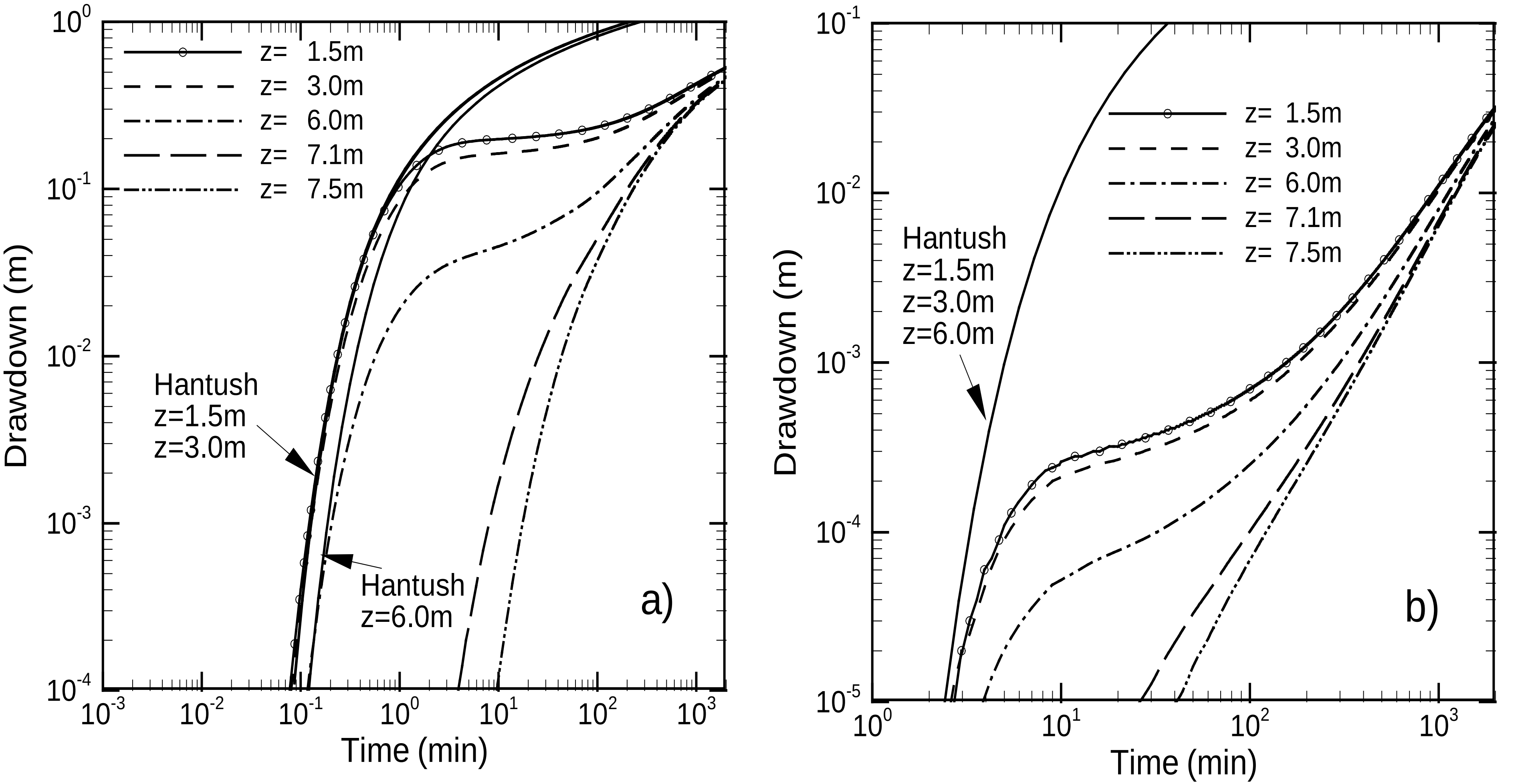

Figure1. Log-log drawdown time curves at five different elevations (z =1.5, 3.0, 6.0, 7.1, 7.5 m) at a) r = 5 m and b) r = 30 m. Solid lines denote the results based on the solution by Hantush at three observation elevations in the saturated zone z = 1.5, z = 3.0, z = 6.0m. In Figure a, the difference between the Hantush solution at z=1.5 m and z=3.0 m is not distinguishable. In Figure b, the solutions are the same at all three elevations.

Previous Study

- Boulton[1954, 1963] use an empirical delay coefficient to the specific yield term to represent the slow water release process.

$$\frac{\partial^2 s}{\partial r^2}+\frac{1}{r}\frac{\partial s}{\partial r}=\frac{S}{T}\frac{\partial s}{\partial t}+\alpha\frac{S_y}{T}\int_0^t\frac{\partial s}{\partial t}e^{-\alpha(t-\gamma)}d\gamma$$

Based on the concept of instantaneous and complete drainage at the water table, Neuman [1972] use downward hydraulic head gradient below the water table to produce the S-shaped curve.

The free-surface boundary condition for the water table

Delayed Water Table response

$$K_r \frac{\partial s}{\partial r}\mathbf{n}_r + K_Z \frac{\partial s}{\partial z}\mathbf{n}_Z = \left(S_y \frac{\partial \xi}{\partial t} - I \right)\mathbf{n}_Z$$

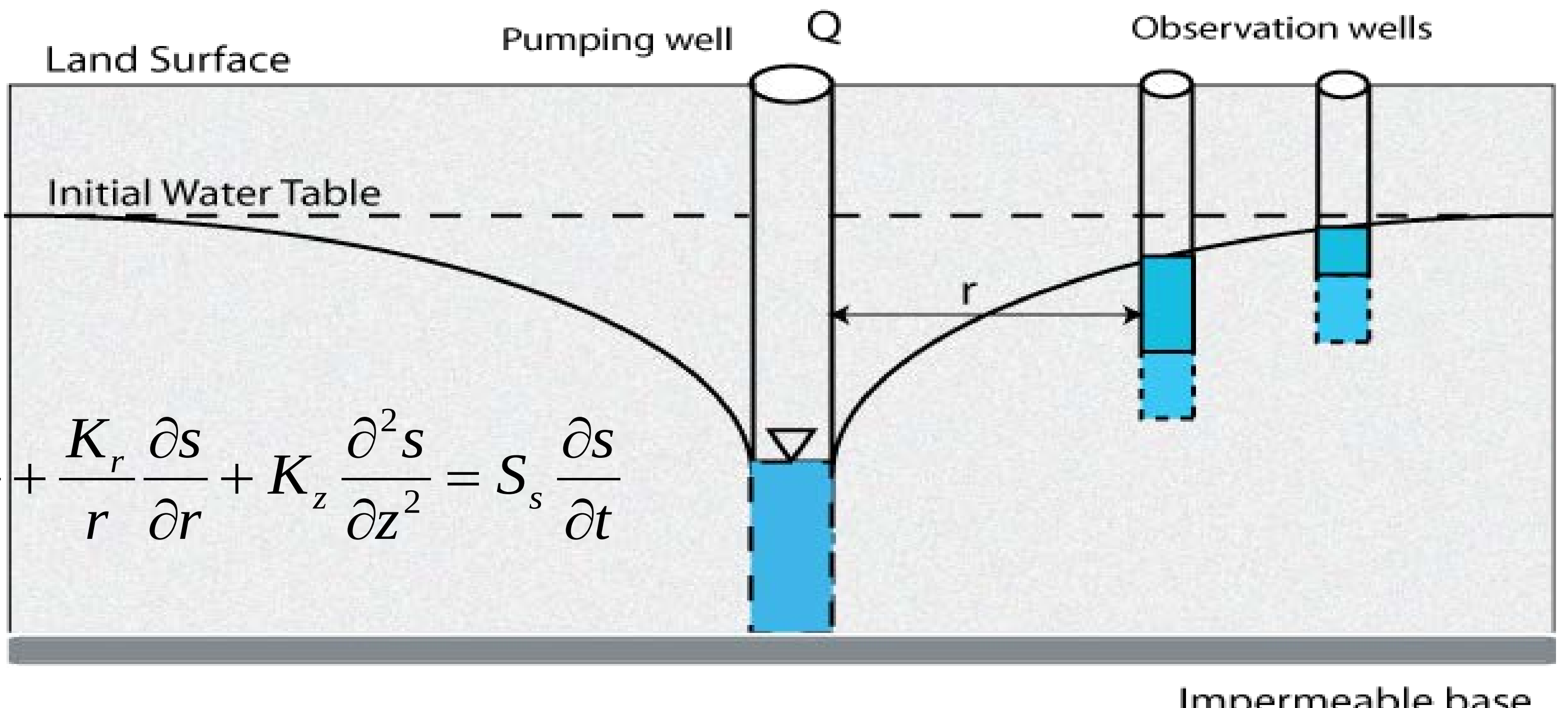

$$K_r \frac{\partial^2 s}{\partial r^2} + \frac{K_r}{r}\frac{\partial s}{\partial r} + K_z \frac{\partial^2 s}{\partial z^2} = S_s \frac{\partial s}{\partial t}$$

S-shaped Drawdown Curve

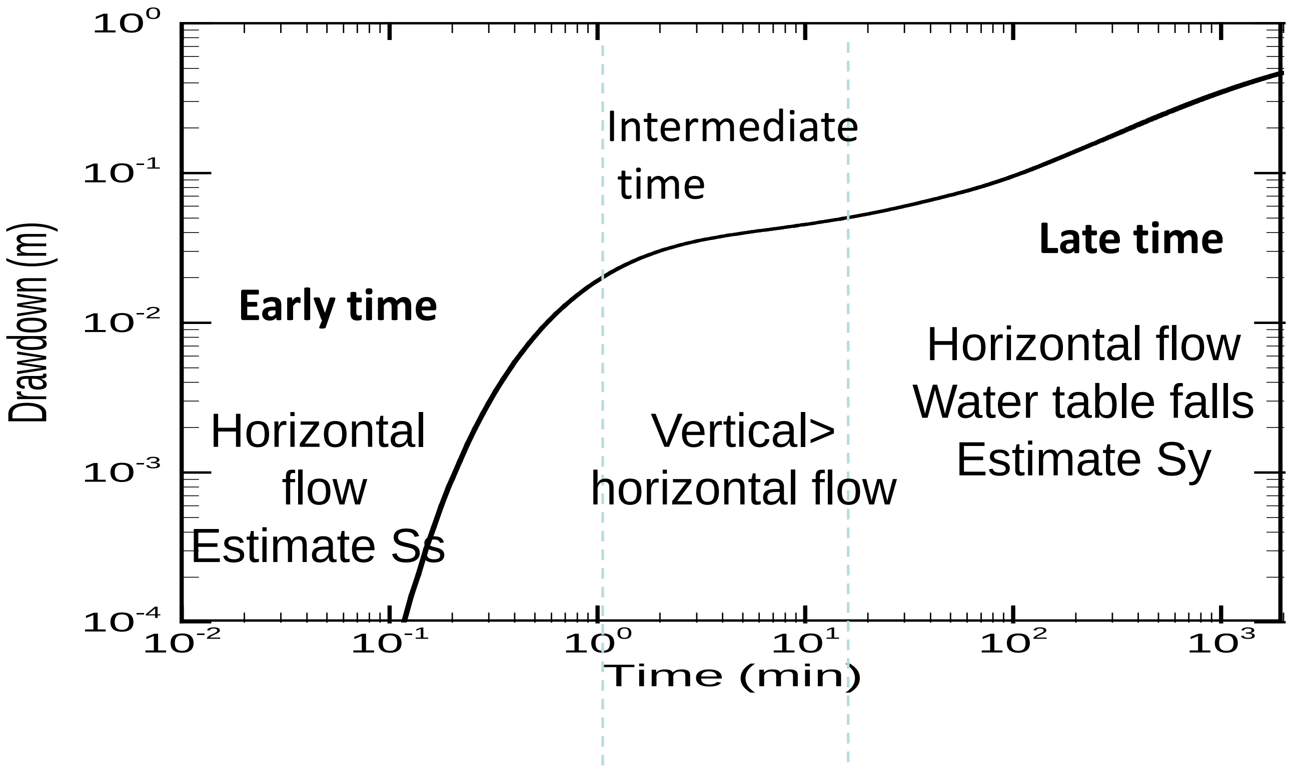

- Nwankwor et al. [1992] explained the S-shaped time-drawdown behavior as a consequence of changes in vertical hydraulic gradients and expansion of capillary fringe.
- Narasimhan and Zhu [1993] advocated that unsaturated zone above the water table is important. It must be included in the analysis.
- Mathias and Butler[2006], Tartakovsky and Neuman [2007] includes the unsaturated flow to improve the analytical solution.

Rate Change of Storage

$$\nabla \cdot [K(h,\mathbf{x})\nabla(h+z)] = \omega S_s(\mathbf{x})\frac{\partial h}{\partial t} + \frac{\partial \theta}{\partial t} = \left(\omega S_s(\mathbf{x}) + C(h,\mathbf{x})\right)\frac{\partial h}{\partial t}$$

$$\Omega = \left(\omega S_s(\mathbf{x}) + C(h,\mathbf{x})\right)\frac{\partial h}{\partial t}$$

- Rate change in storage represents the net flux in a unit volume of the porous media per time!

Ss: expansion of water and compaction of porous media.

C (h): drainage of water from pores.

Rate Change of Storage

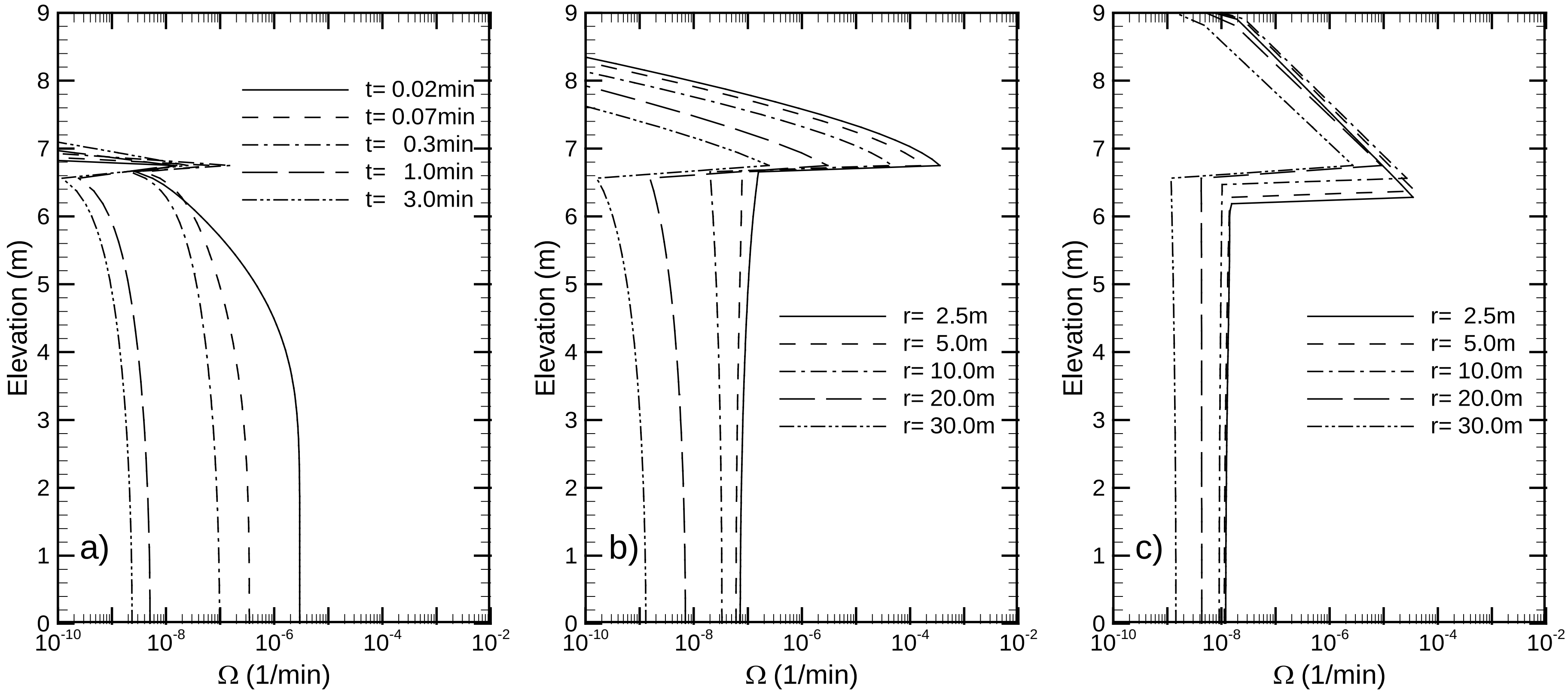

Early time

Elastic effect

Intermediate time

Drainage of initial unsaturated zone

Late time

Drainage of pores falling water table

1D Example

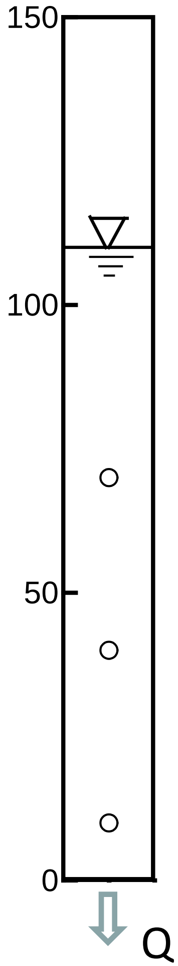

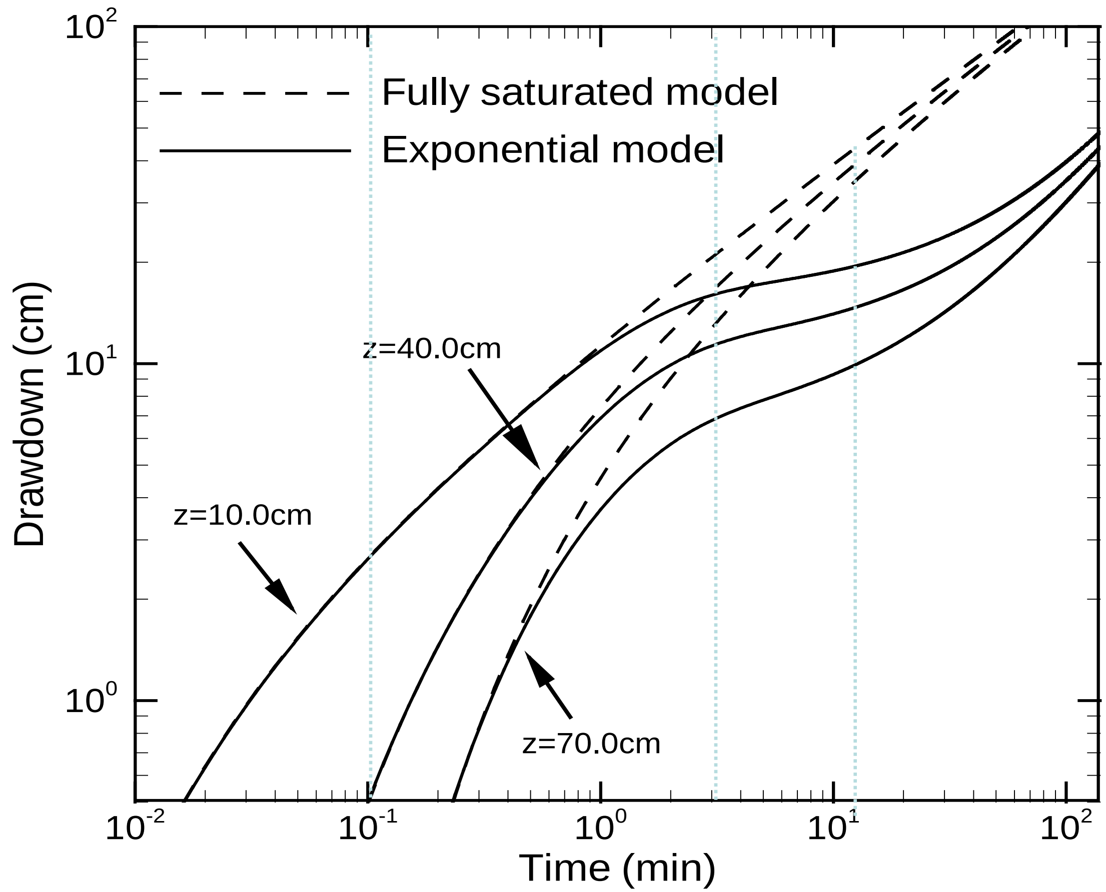

Drawdown curve

1D Example

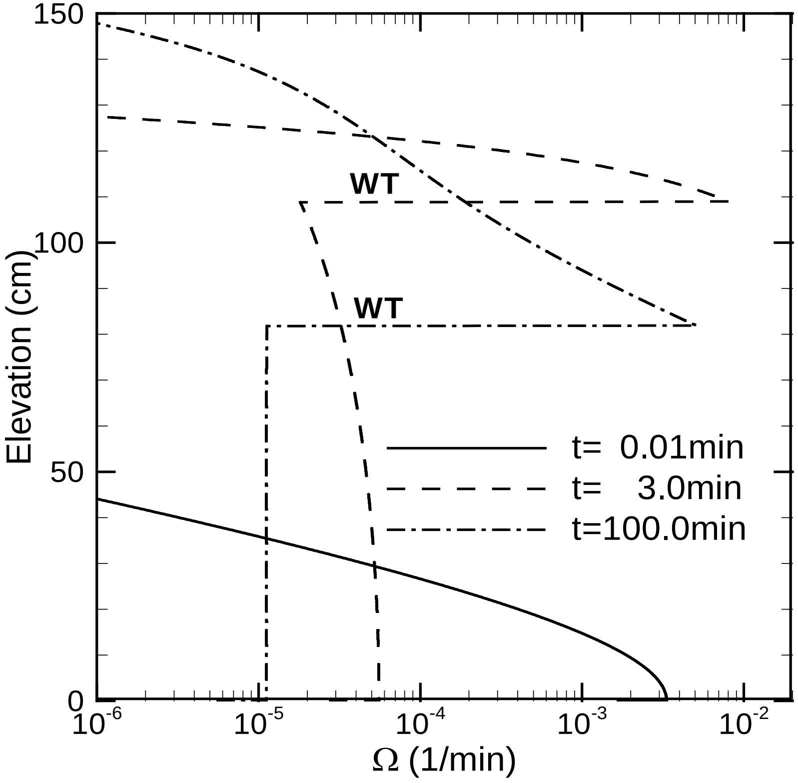

Rate change of storage

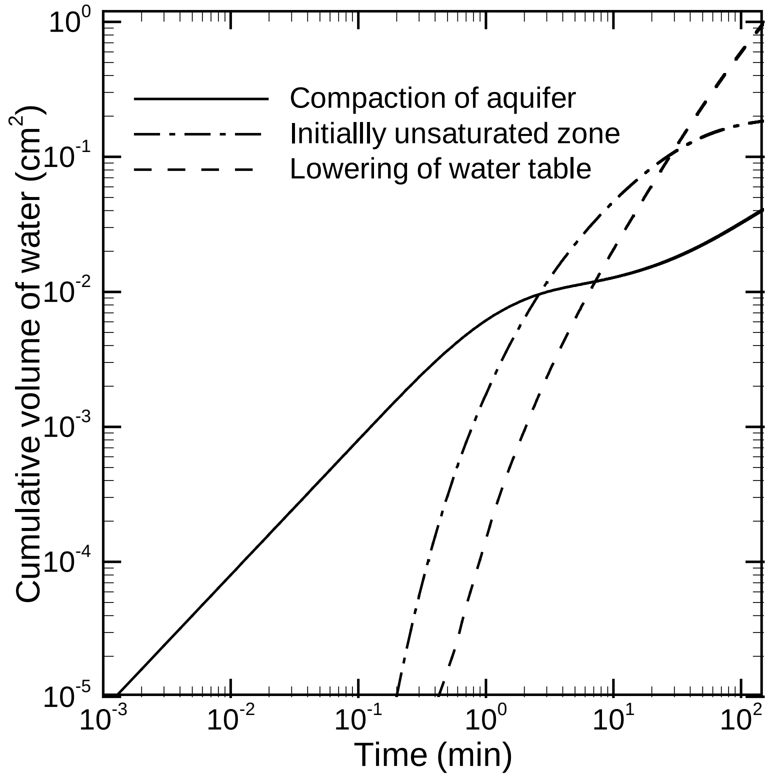

Cumulative water release

Effect of Initial Unsaturated Zone

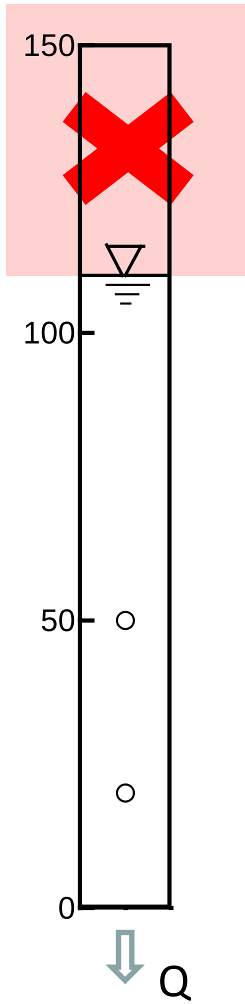

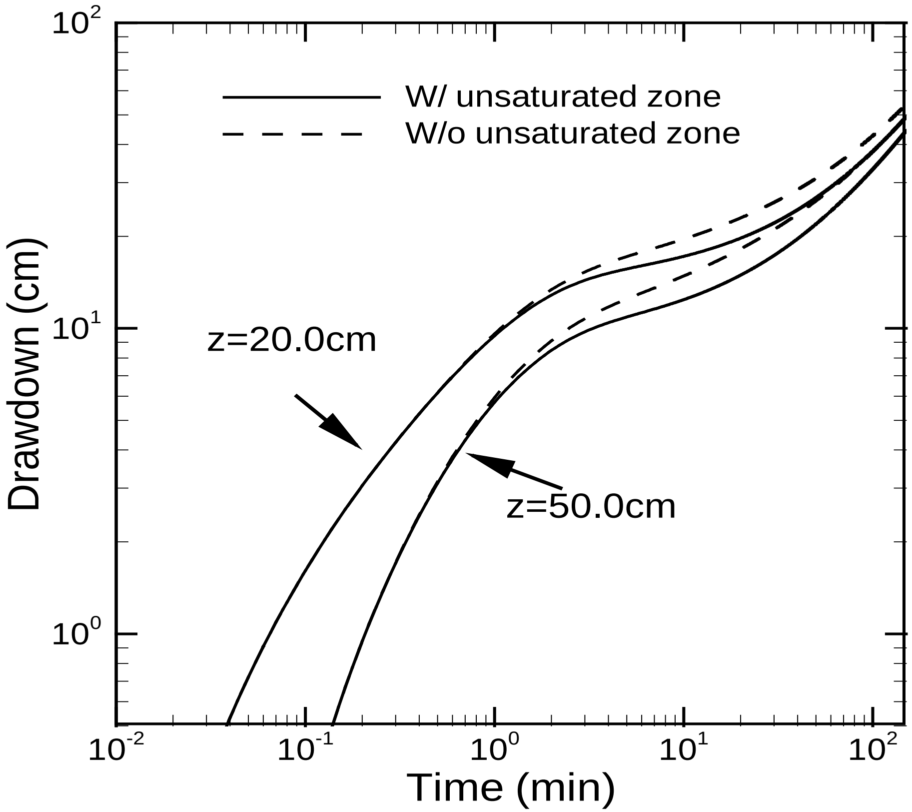

Drawdown curve

What is the Cause of S-shaped drawdown-time curve ?

It is merely the **transition of water release mechanisms during vertical flow** from 1) expansion of water/compaction of the porous medium to 2) drainage of water from the unsaturated zone above initial water table, and 3) initially saturated pores as the water table falls during the pumping of the aquifer.

The widely accepted terms “delayed yield” and “delayed water table response” do not elucidate the transition of the two water release mechanisms and these terms may be misleading!

Effect of Parameter Heterogeneity

- 1st order approximation

$$H(\mathbf{x},t) = \overline{H}(\mathbf{x},t) + p(\mathbf{x},t) = \overline{H}(\mathbf{x},t) + f(\mathbf{x}) \cdot \frac{\partial H}{\partial \ln K_S(\mathbf{x})} + s(\mathbf{x}) \cdot \frac{\partial H}{\partial \ln S_S(\mathbf{x})} + a(\mathbf{x}) \cdot \frac{\partial H}{\partial \ln \alpha(\mathbf{x})} +$$

$$b(\mathbf{x}) \cdot \frac{\partial H}{\partial \ln \beta(\mathbf{x})} + t_s(\mathbf{x}) \cdot \frac{\partial H}{\partial \ln \theta_s(\mathbf{x})} + t_r(\mathbf{x}) \cdot \frac{\partial H}{\partial \ln \theta_r(\mathbf{x})}$$

- Head covariance

$$\mathbf{R}_{pp} = \mathbf{J}_{pf}\mathbf{R}_{ff}\mathbf{J}_{pf}^{T} + \mathbf{J}_{ps}\mathbf{R}_{ss}\mathbf{J}_{ps}^{T} + \mathbf{J}_{pa}\mathbf{R}_{aa}\mathbf{J}_{pa}^{T} + \mathbf{J}_{pb}\mathbf{R}_{bb}\mathbf{J}_{pb}^{T} + \mathbf{J}_{pt_s}\mathbf{R}_{t_st_s}\mathbf{J}_{pt_s}^{T} + \mathbf{J}_{pt_r}\mathbf{R}_{t_rt_r}\mathbf{J}_{pt_r}^{T}$$

- Cross correlation

$$\rho_{pf}(\mathbf{x}_i, \mathbf{x}_j, t) = \frac{\mathbf{R}_{pf}(\mathbf{x}_i, \mathbf{x}_j, t)}{\sigma_p(\mathbf{x}_i, t)\sigma_f} = \frac{\mathbf{J}_{pf}(\mathbf{x}_i, \mathbf{x}_j, t)\mathbf{R}_{ff}(\mathbf{x}_i, \mathbf{x}_j)}{\sigma_p(\mathbf{x}_i, t)\sigma_f}$$

Effect of Parameter Heterogeneity

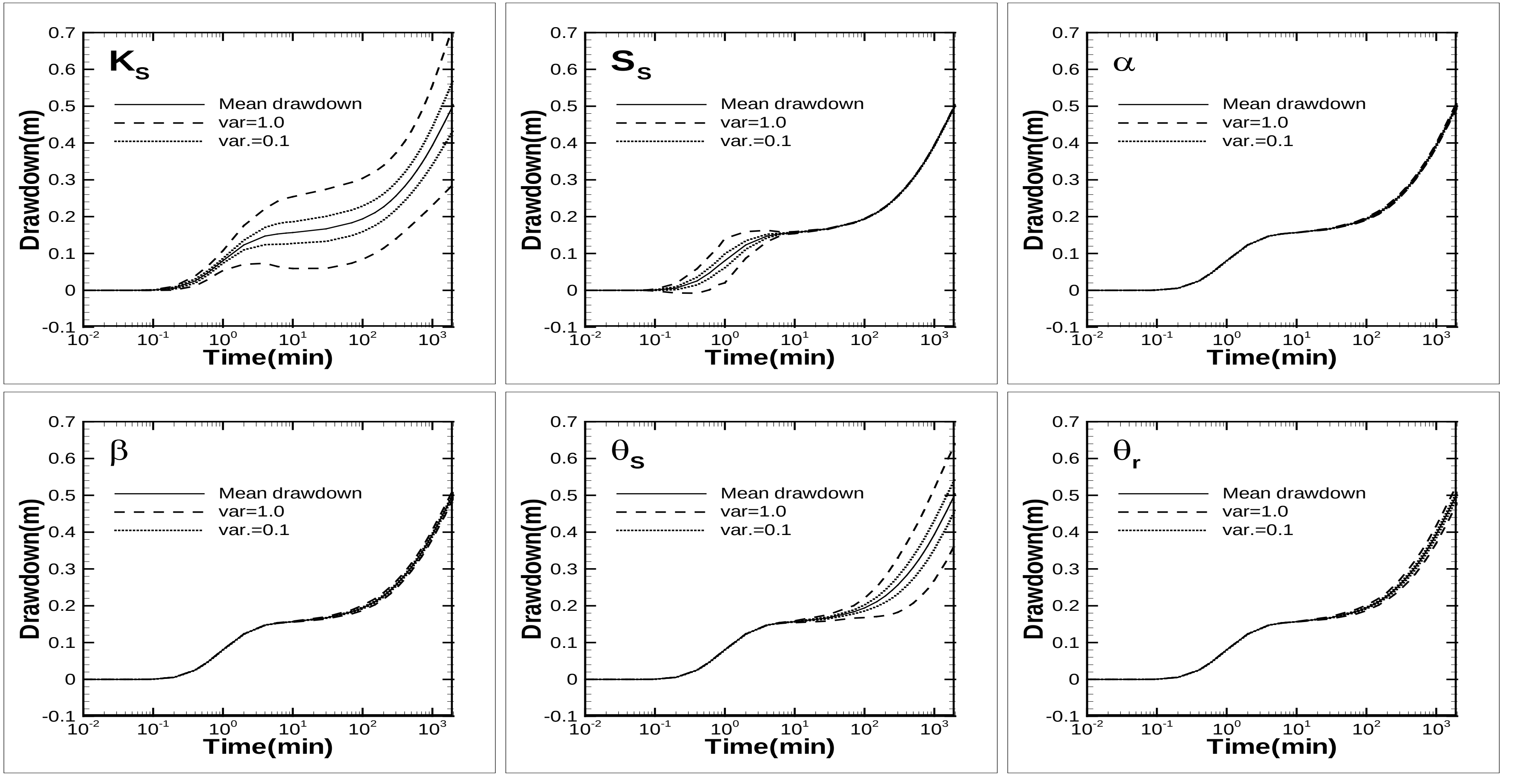

The S-shaped drawdown-time curve is sensitive to the spatial variability of K_s, S_s, and θ_s.

Cross Correlation Analysis

Between head and *Ks*

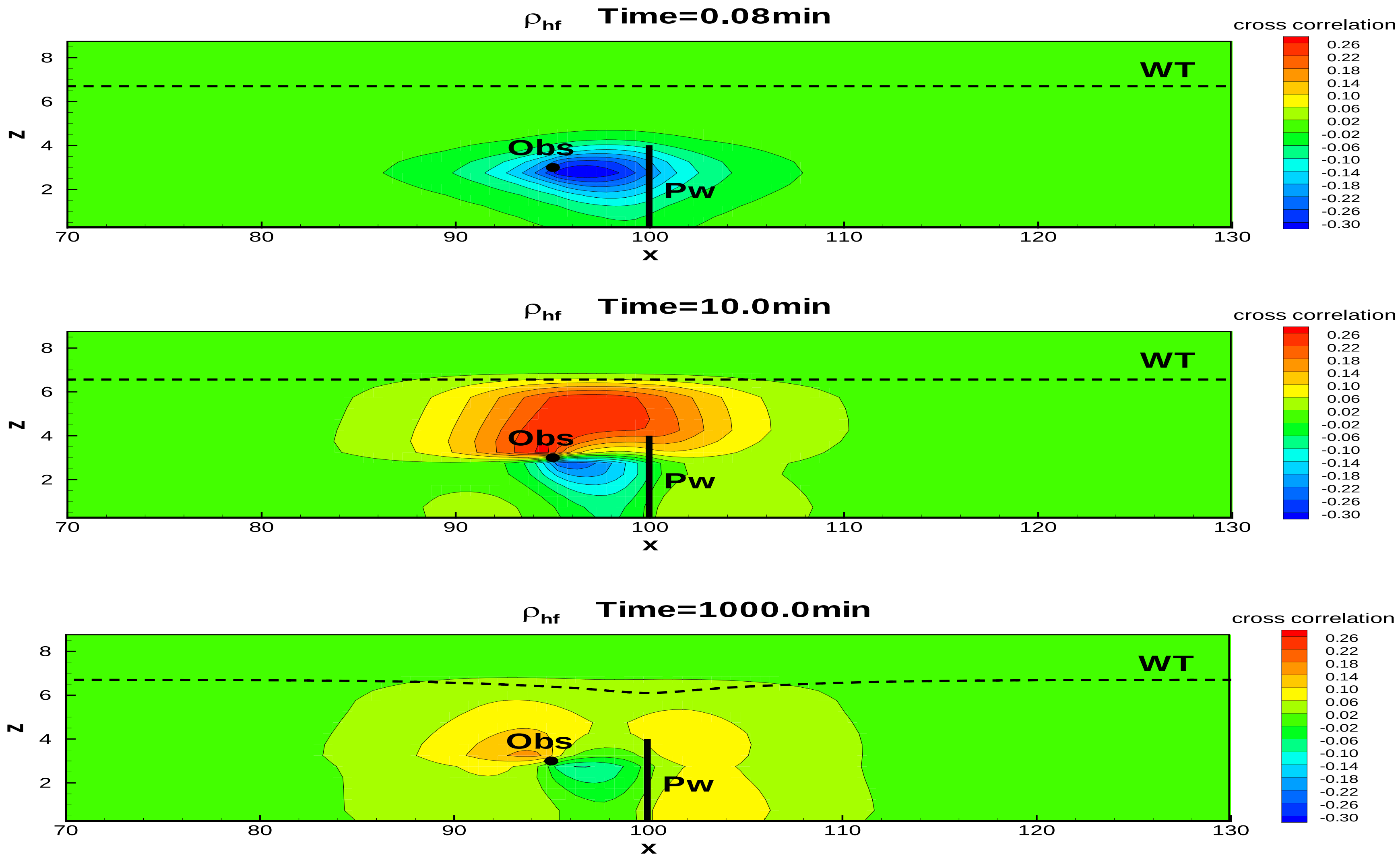

Cross Correlation Analysis

Between head and S_s

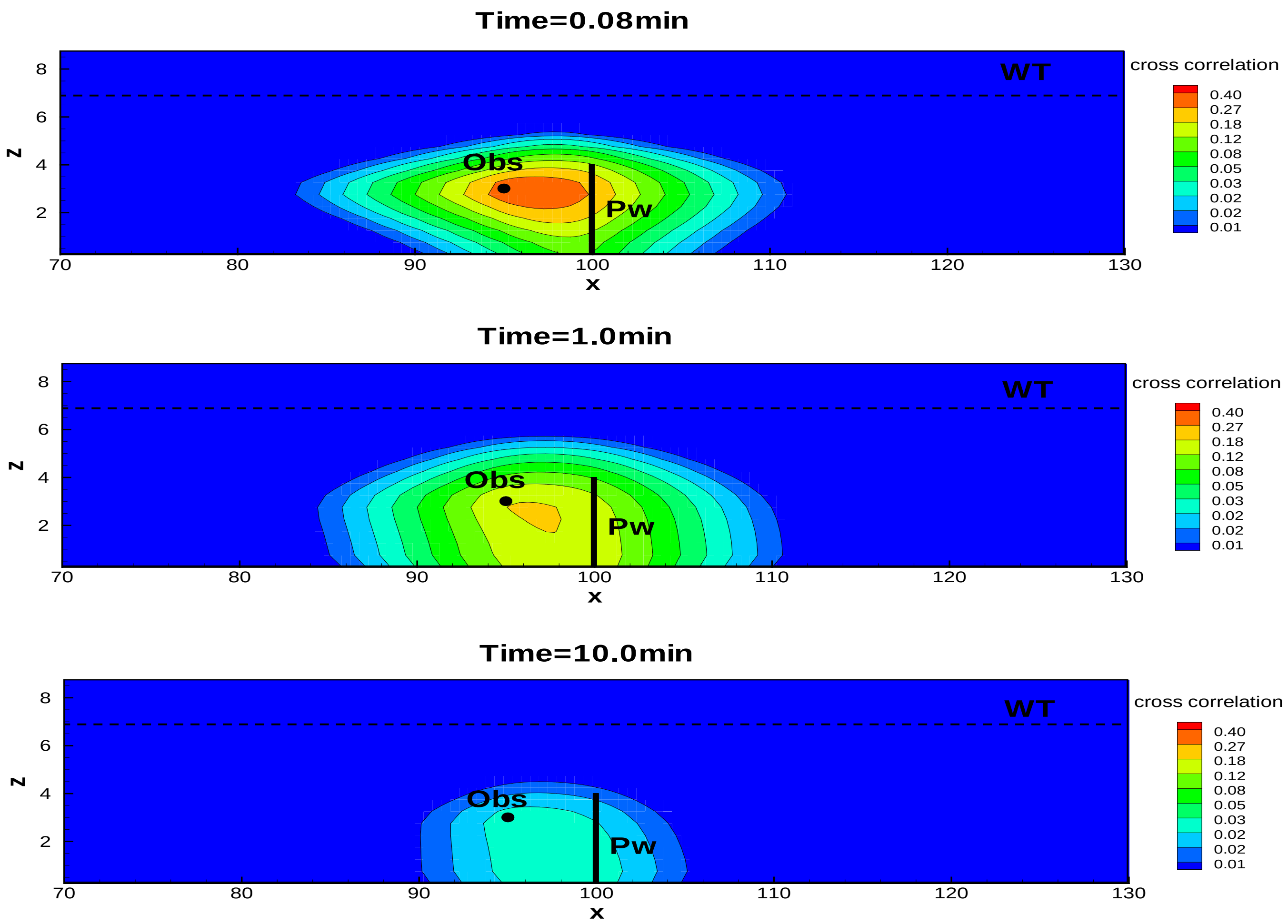

Cross Correlation Analysis

Between head and θ_s

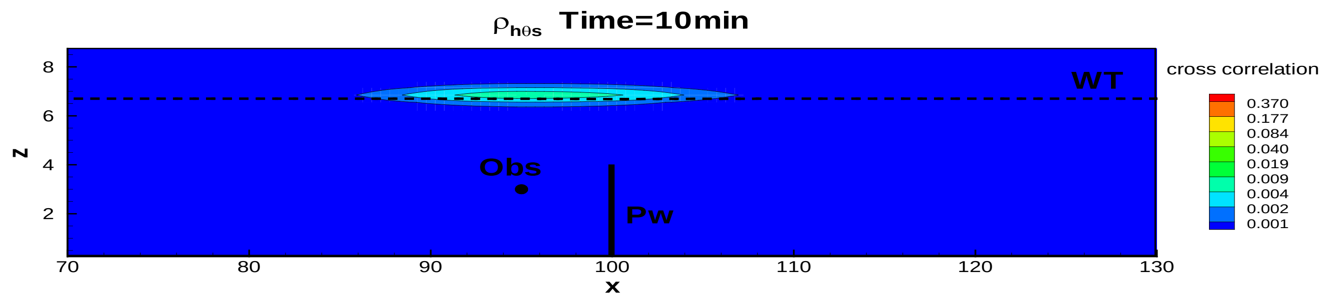

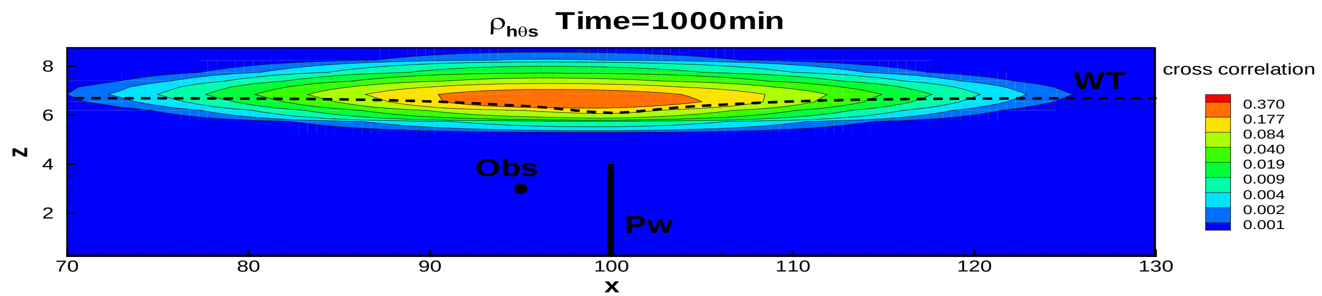

Cross correlation analysis shows an observation location in the aquifer is not equally influenced by heterogeneity everywhere in the aquifer. As a consequence, applications of a model assuming homogeneity to estimation of parameters may require a large number of spatial observations in order to yield representative parameter values.

Conclusion

- Transition of water release mechanisms and vertical flow explain the S-shaped drawdown curve.
- Heterogeneous variably saturated governing equation

$$\nabla \cdot [K(h,\mathbf{x})\nabla(h+z)] = \omega S_s(\mathbf{x})\frac{\partial h}{\partial t} + \frac{\partial \theta}{\partial t} = \left(\omega S_s(\mathbf{x}) + C(h,\mathbf{x})\right)\frac{\partial h}{\partial t}$$

  considers the transition of water release mechanisms and heterogeneity would provide a more realistic representation of flow processes in unconfined aquifer.
- Variability in the saturated zone parameters has greater impacts than that in the vadose zone on the S curve.
- Hydraulic tomography would be a viable approach for delineating heterogeneity in unconfined aquifers.

FLOW TO A WELL IN A HETEROGENEOUS UNCONFINED AQUIFER: INSIGHTS FROM INTERMEDIATE SCALE SANDBOX EXPERIMENTS

Steven J. Berg and Walter A. Illman
University of Waterloo Canada

Figure 1: Photograph of the sandbox showing all sensor locations (● = pressure transducers; ● without pressure transducers; ○ = tensiometers; and **x** = water content probes) and the various layers that were packed. Sensor locations are approximate.

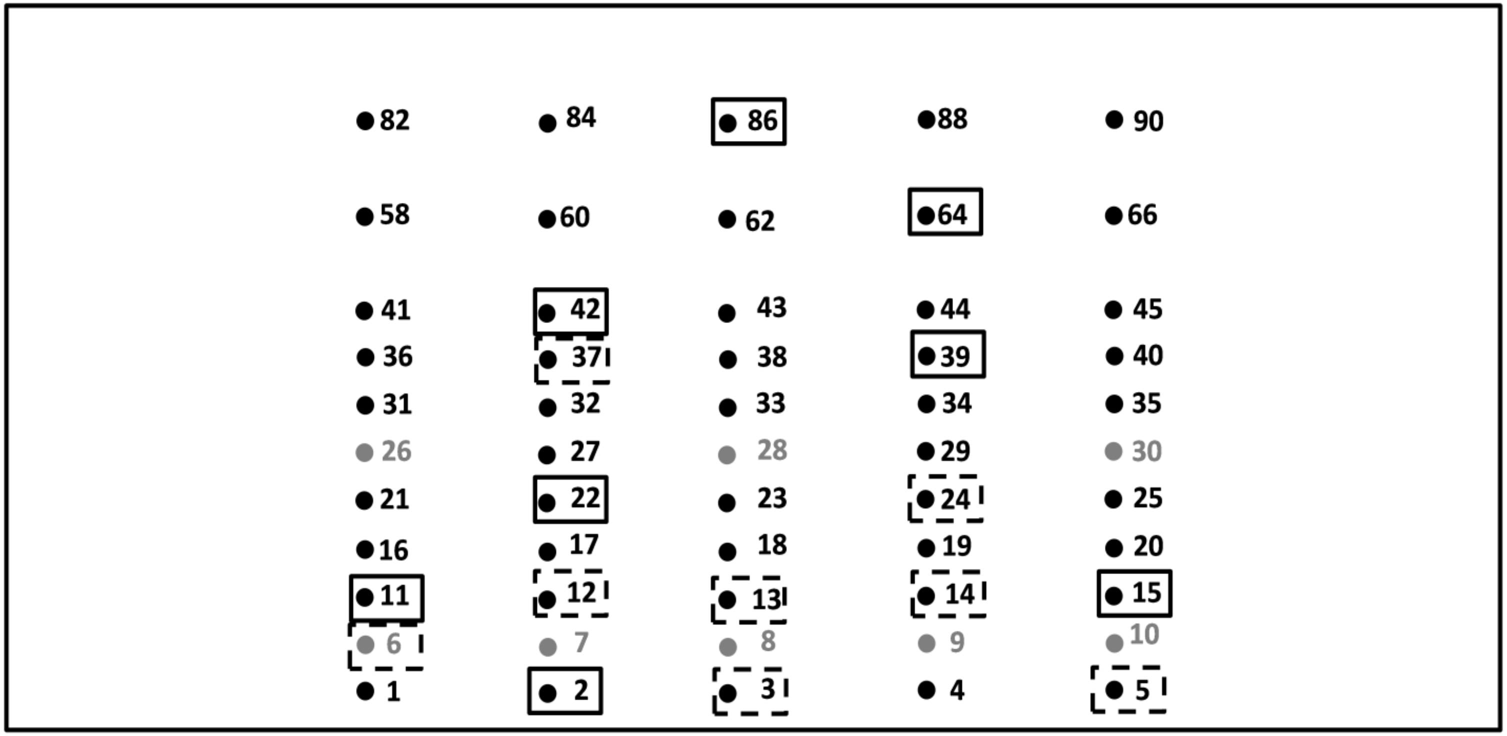

Figure 2: Schematic diagram showing the ports that were pumped for the cross-hole pumping tests. Solid black circles represent locations of pressure transducers and solid grey circles represent ports that were not instrumented. Solid squares are pumping locations used for the estimation of homogeneous and heterogeneous *K* and *Ss* fields. Dashed squares are pumping locations for the validation of the results from transient hydraulic tomography.

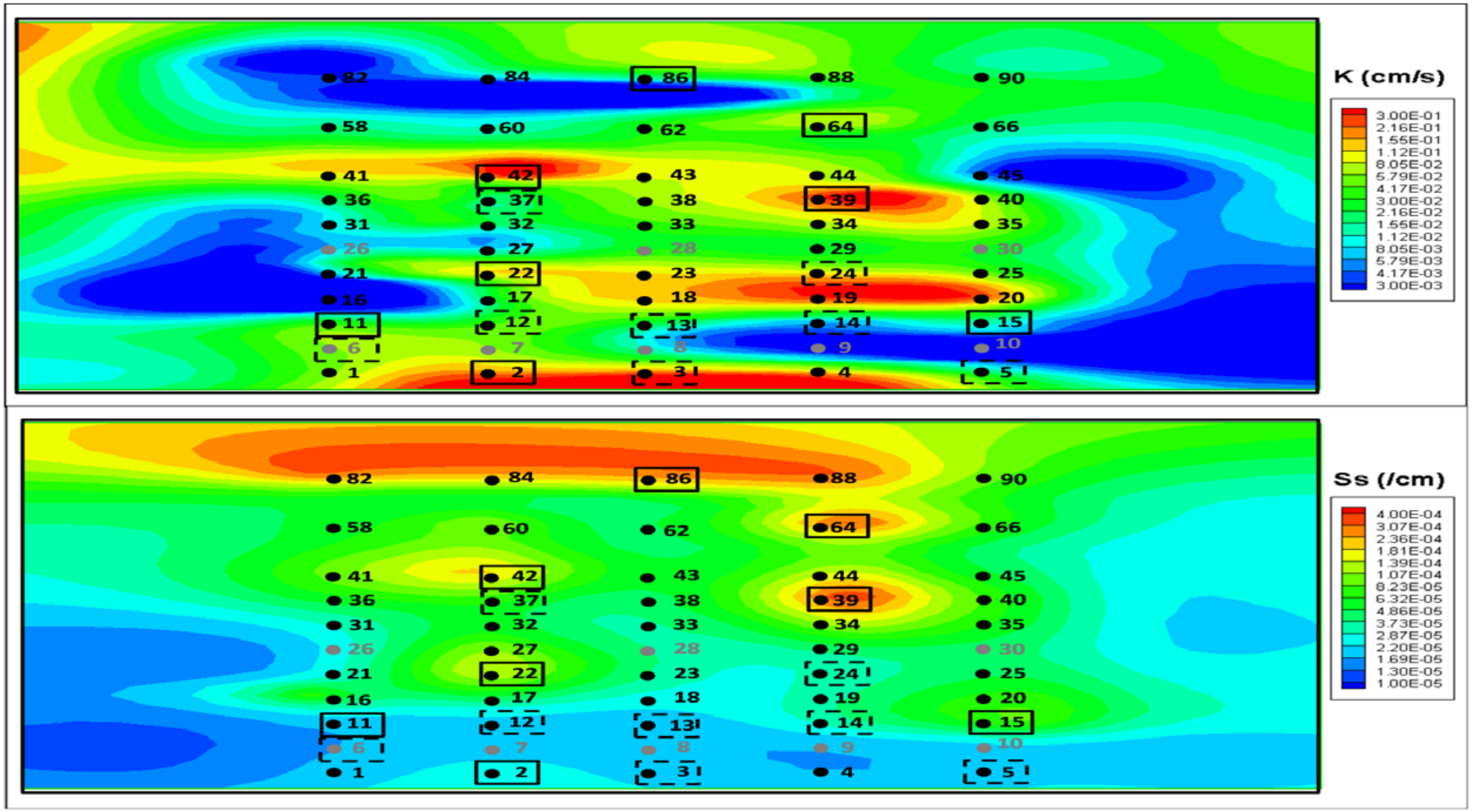

Figure 4: a) *K* and b) *Ss* tomograms computed using the transient hydraulic tomography algorithm of *Zhu and Yeh* [2005] SSLE with 8 cross-hole pumping tests. Solid squares are pumping locations used for transient hydraulic tomography dashed squares are pumping locations for the validation of the results from transient hydraulic tomography.

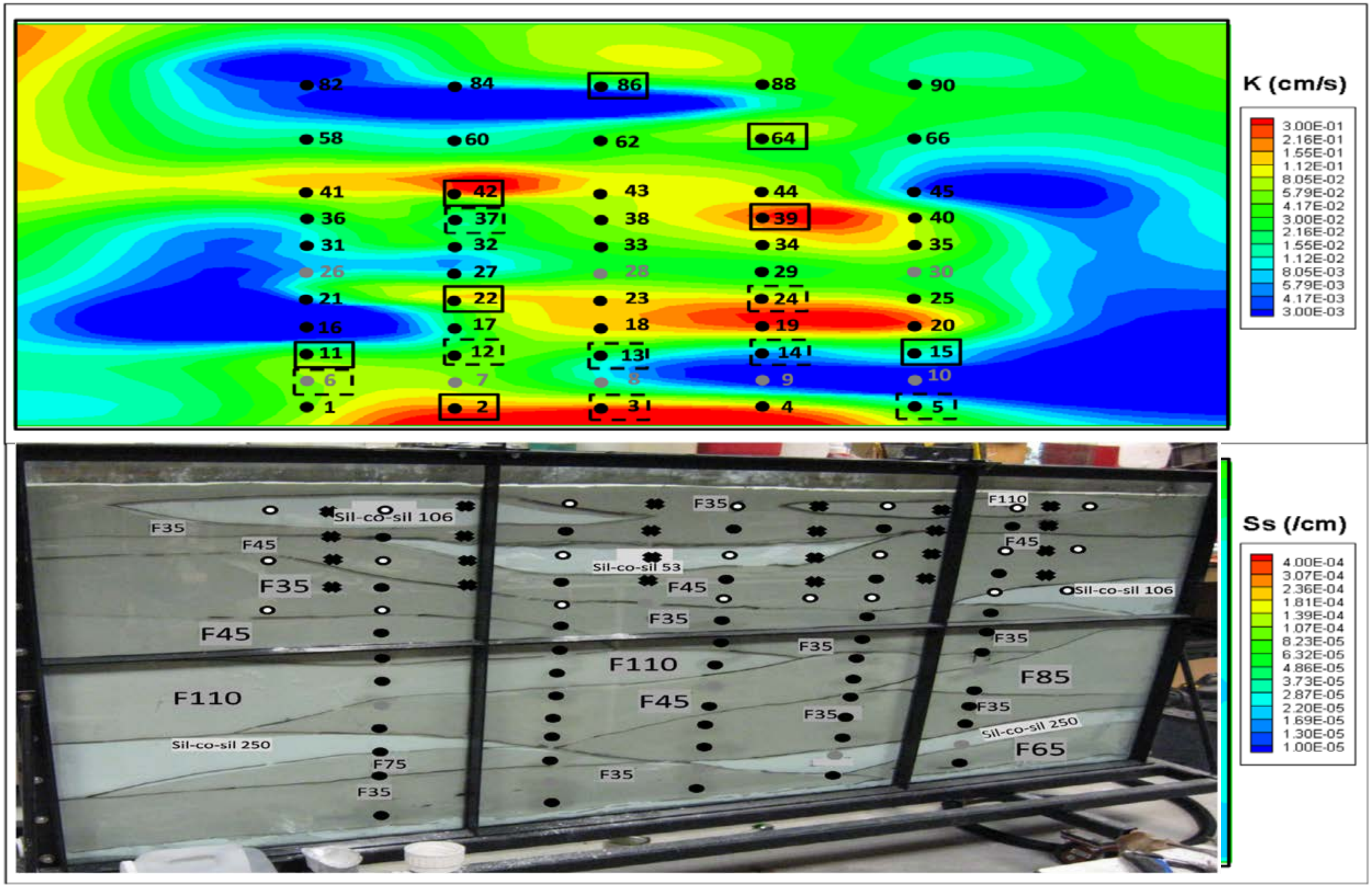

82
84
86
88
90
58
60
62
64
66
41
42
43
44
45
36
37
38
39
40
31
32
33
34
35
26
27
28
29
30
21
22
23
24
25
16
17
18
19
20
11
12
13
14
15
6
7
8
9
10
1
2
3
4
5
K (cm/s)
3.00E-01
2.16E-01
1.55E-01
1.12E-01
8.05E-02
5.79E-02
4.17E-02
3.00E-02
2.16E-02
1.55E-02
1.12E-02
8.05E-03
5.79E-03
4.17E-03
3.00E-03
F35
Sil-co-sil 106
F45
F35
F45
F110
Sil-co-sil 250
F75
F35
F35
Sil-co-sil 53
F45
F35
F110
F45
F35
F35
F35
F110
F45
Sil-co-sil 106
F35
F85
F35
Sil-co-sil 250
F65
Ss (/cm)
4.00E-04
3.07E-04
2.36E-04
1.81E-04
1.39E-04
1.07E-04
8.23E-05
6.32E-05
4.86E-05
3.73E-05
2.87E-05
2.20E-05
1.69E-05
1.30E-05
1.00E-05

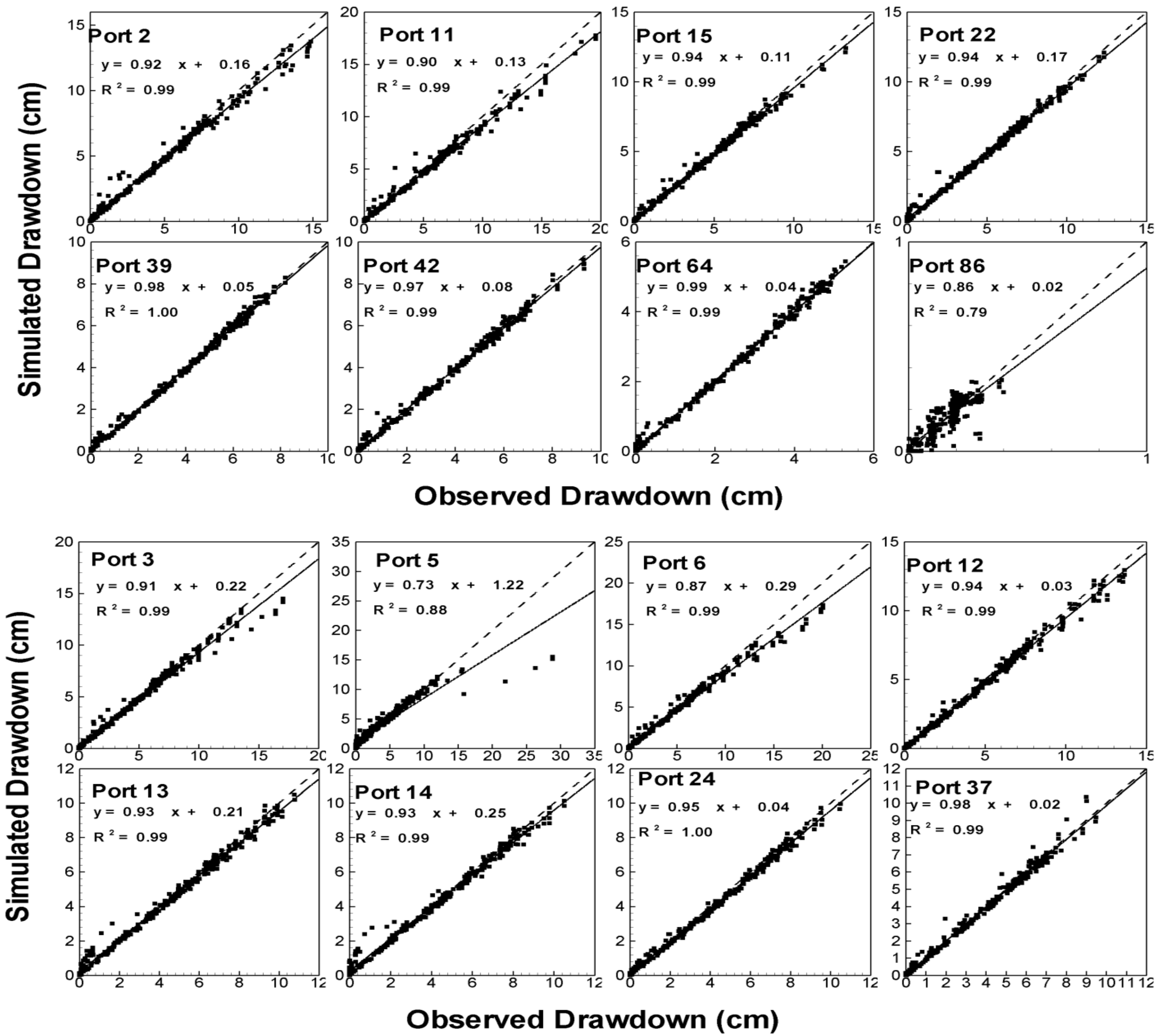

Figure 5: a) Simulated versus observed drawdowns from 8 cross-hole pumping tests used for calibration purposes and b) additional tests used for the validation of the *K* and S_s tomograms.


F35
Sil-co-sil 106
F45
F35
F45
F110
Sil-co-sil 250
F75
F35
F35
Sil-co-sil 53
F45
F35
F110
F45
F35
F35
F35
F110
F45
Sil-co-sil 106
F35
F85
F35
Sil-co-sil 250
F65

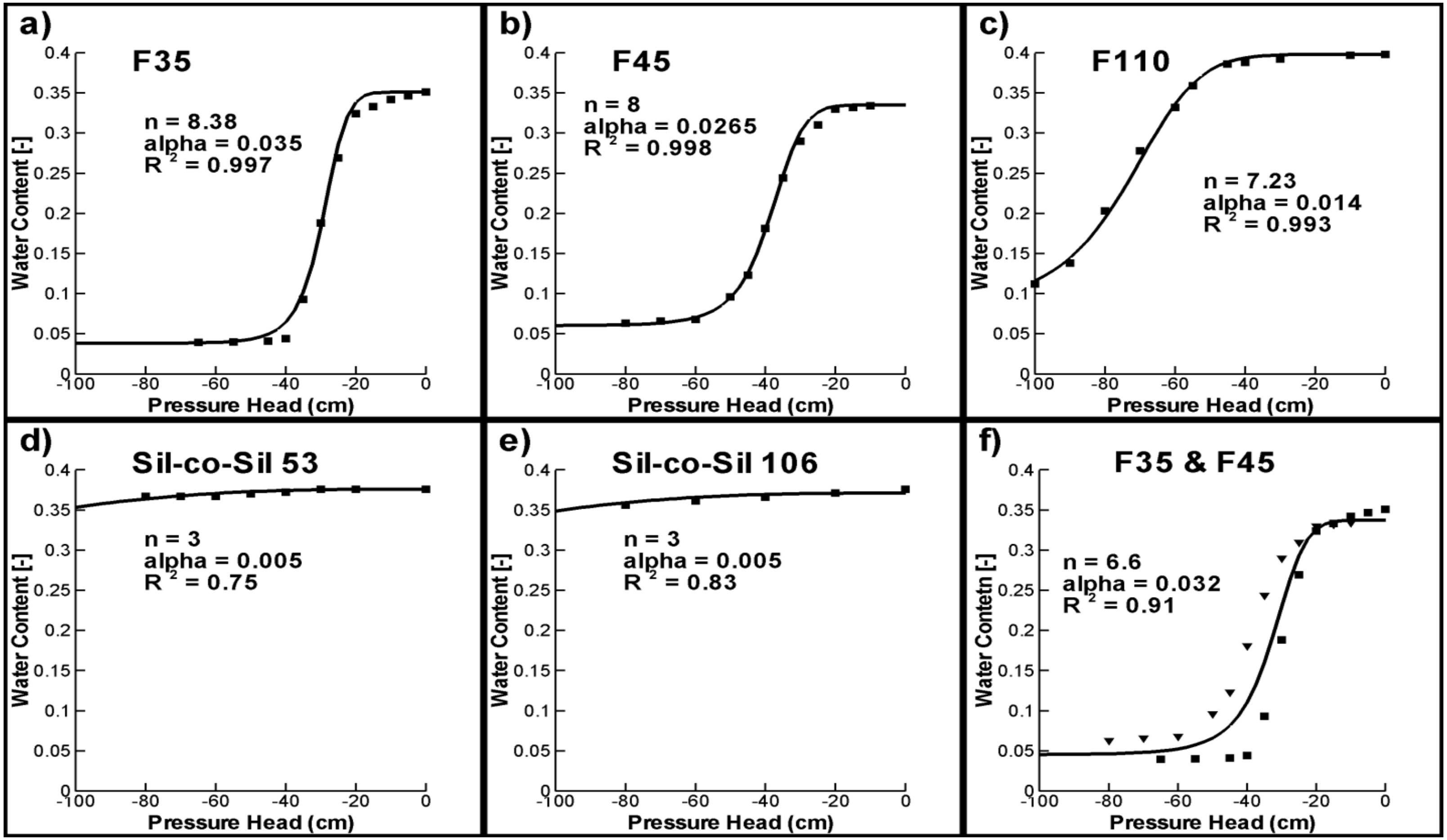

Figure 6: Moisture characteristic curves determined through the hanging column method of: a) F-35; b) F-45; c) F110; d) Sil-co-Sil 53; e) Sil-co-Sil 106; and f) F35 and F45 matched simultaneously. The squares represent F35 and gradient symbols represent F35.

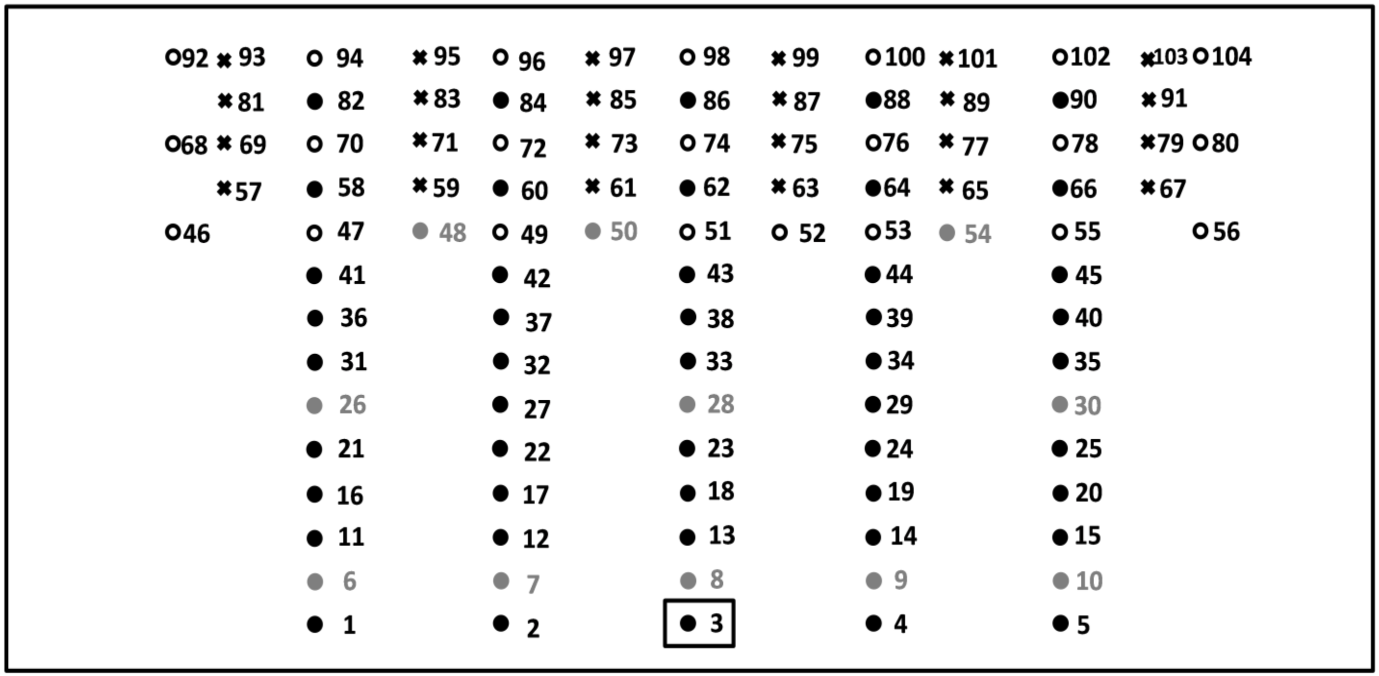

Figure 7: Schematic diagram of the sandbox showing an array of sensors (● = pressure transducers; ● = port without pressure transducers; ○ = tensiometers; and **x** = water content sensors) utilized to monitor the pumping test in a heterogeneous unconfined aquifer. The box indicates the port at which the unconfined pumping test was performed.

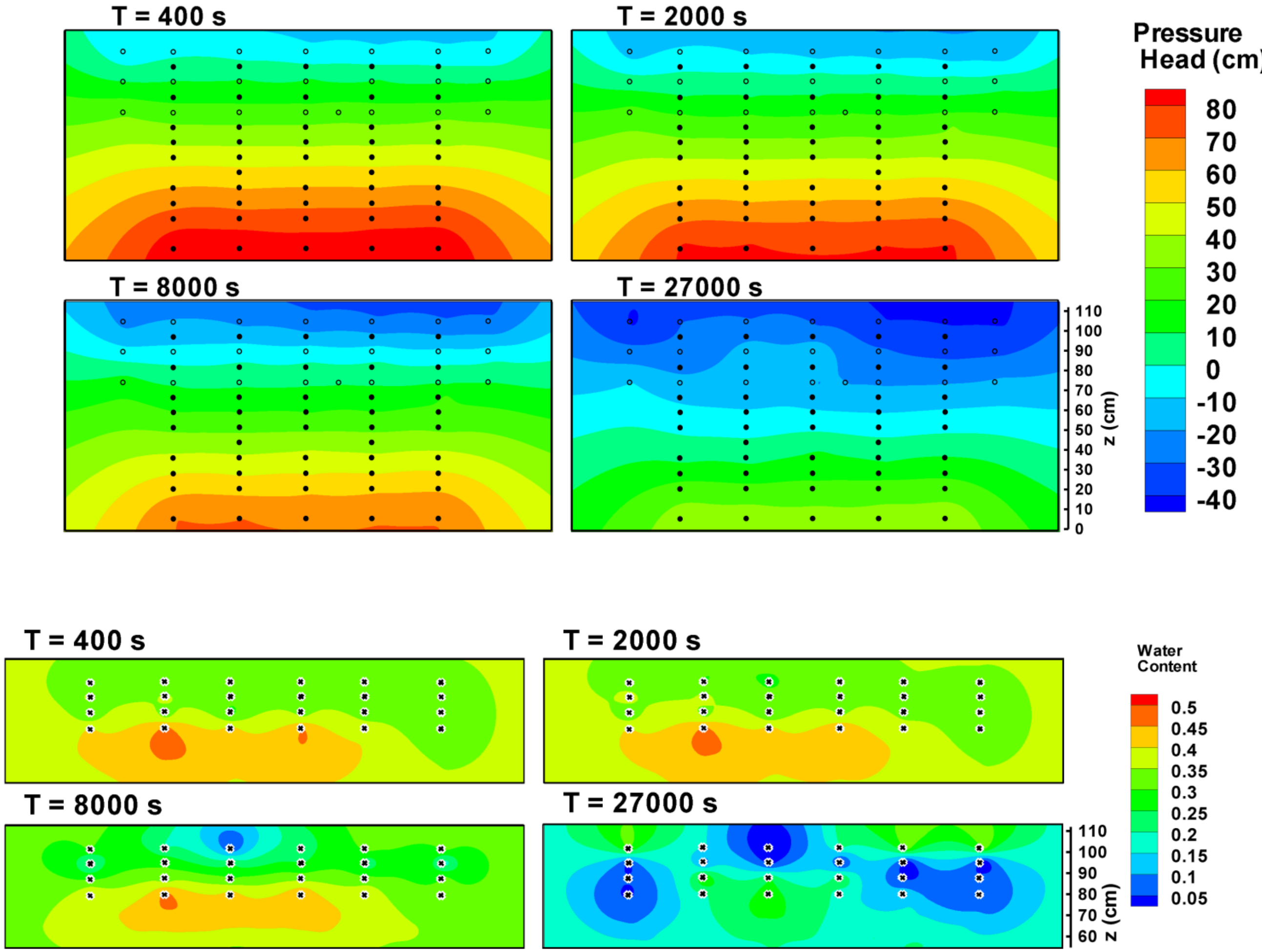

Figure 9: Spatial distribution of: a) pressure head and b) volumetric water content in the upper half of the sandbox with time during the unconfined aquifer pumping test at port 3. Symbols indicate the position of various sensors used to monitor the pumping test (● = pressure transducers; ○ = tensiometers; and **x** = water content sensors)).

Case 1.

Homogeneous vadose
Zone and homogeneous
aquifer

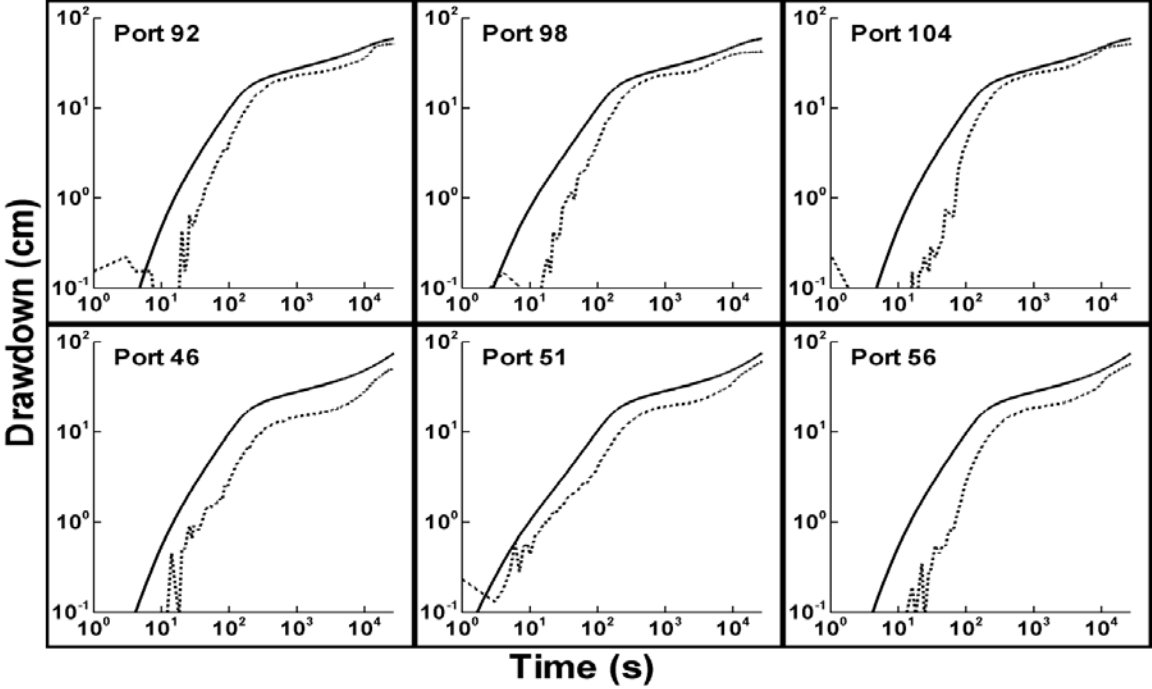

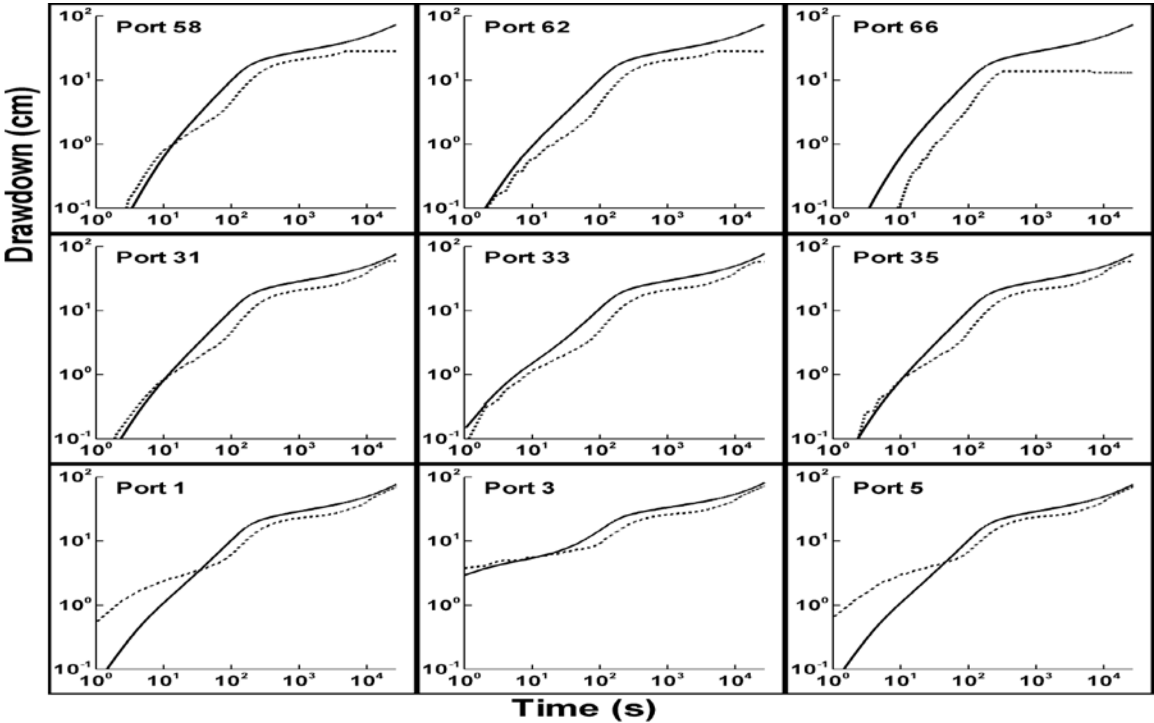

Figure 10: Simulated (solid line) and observed (dashed line) drawdown from selected: a) pressure transducers; and, b) tensiometers during the unconfined aquifer pumping test (Case 1). A comparison at all ports is available online as Figure S2.

Case 2.

Homogeneous vadose
Zone and heterogeneous
 aquifer

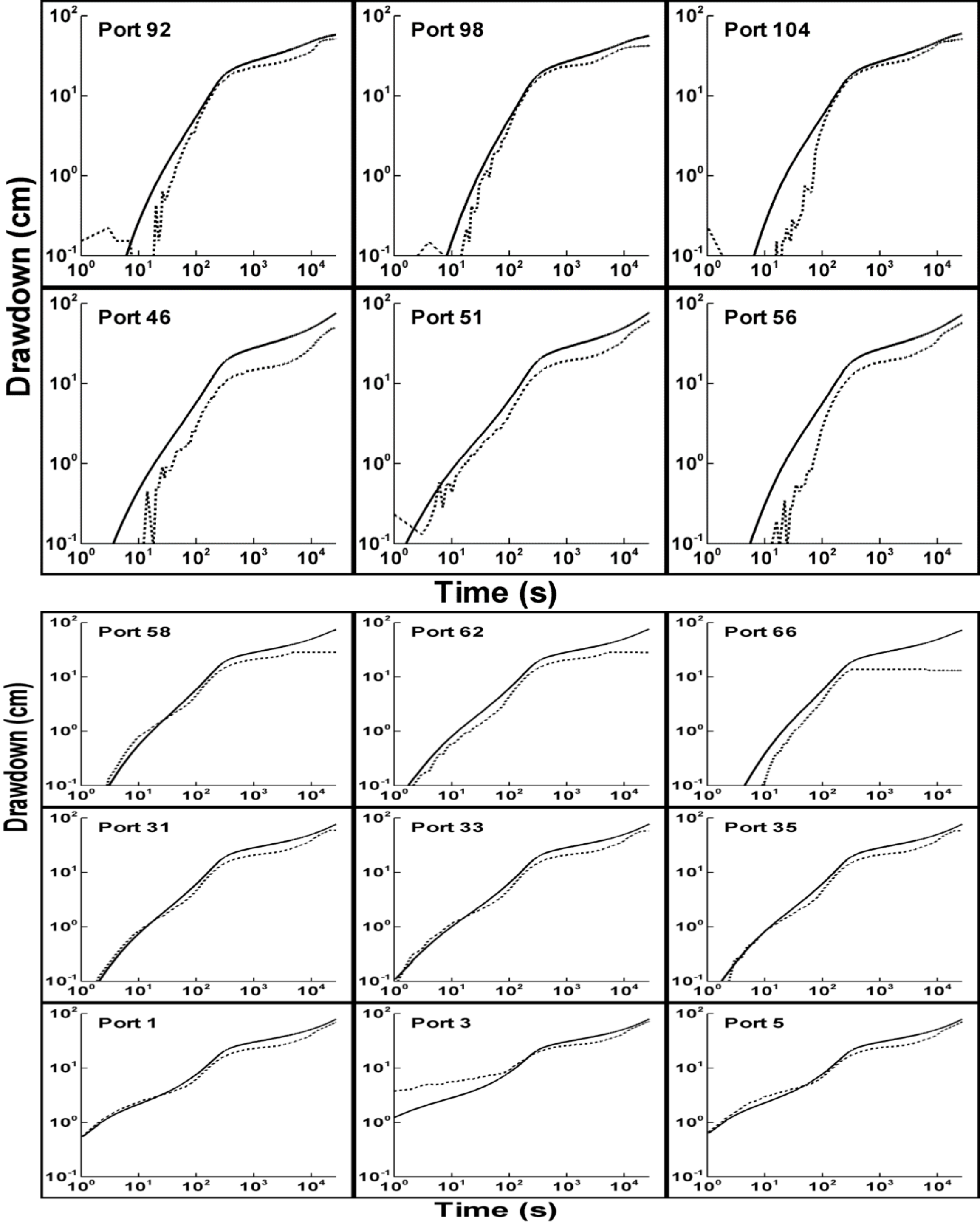

Figure 11: Simulated (solid line) and observed (dashed line) drawdown from selected: a) pressure transducers; and, b) tensiometers during the unconfined aquifer pumping test (Case 2). A comparison at all ports is available online as Figure S3.

Case 3.

Heterogeneous vadose
Zone and aquifer

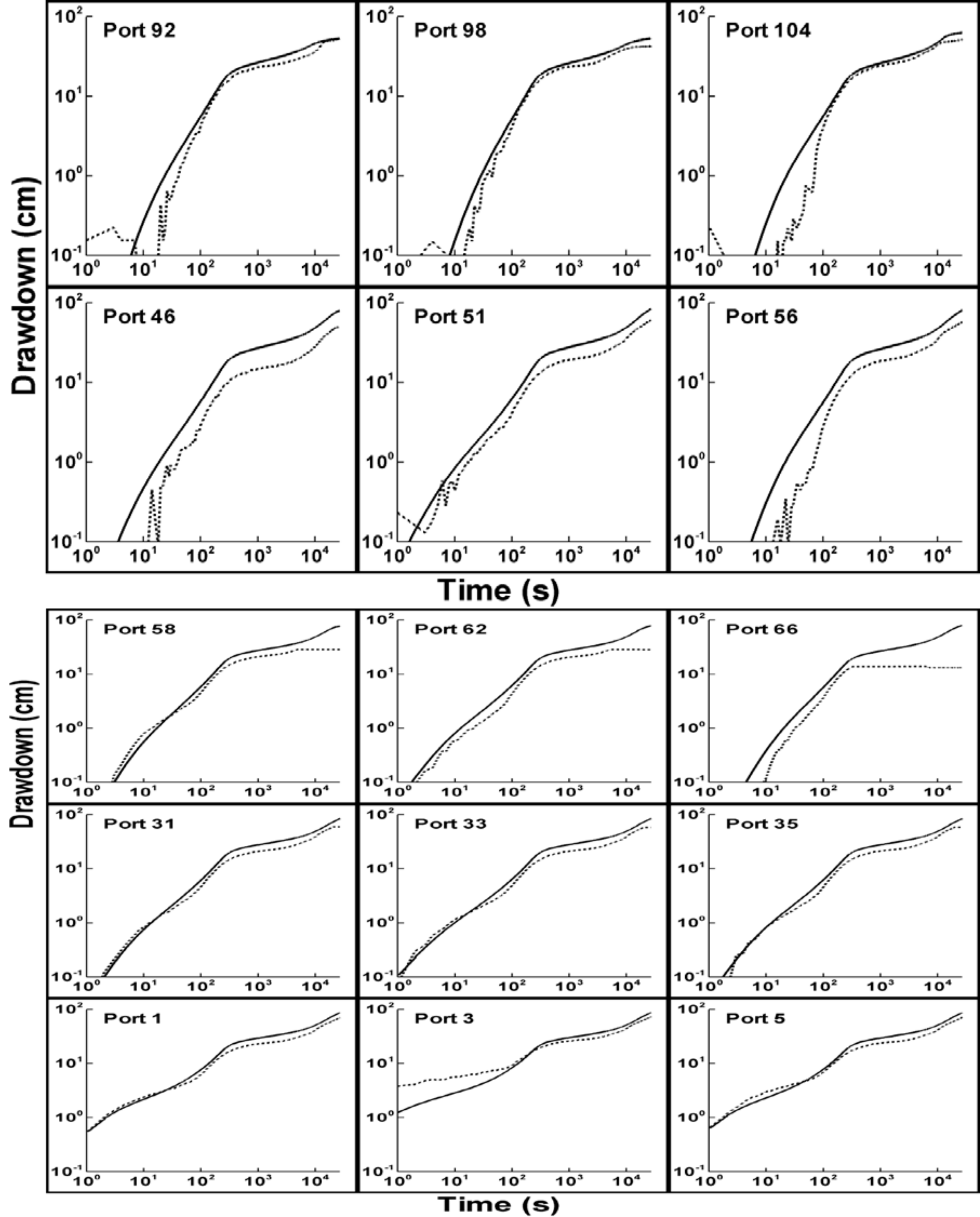

Figure 12: Simulated (solid line) and observed (dashed line) drawdown from selected: a) pressure transducers; and, b) tensiometers during the unconfined aquifer
pumping test (Case 3). A comparison at all ports is available online as Figure S4.